Available online at www.sciencedirect.com
ScienceDirect
Tetrahedron: Asymmetry
Tetrahedron: *Asymmetry* 19 (2008) 124–130

Chiral recognition of dipeptides in bio-membrane models: the role of amphiphile hydrophobic chains

Cecilia Bombelli,[a] Stefano Borocci,[b,*] Oscar Cruciani,[c] Giovanna Mancini,[a,*] Donato Monti,[d] Anna Laura Segre,[c] Alessandro Sorrenti[a] and Mariano Venanzi[d]

[a]*CNR, Istituto di Metodologie Chimiche and Dipartimento di Chimica, Università degli Studi di Roma 'La Sapienza', P.le A. Moro 5, 00185 Roma, Italy*
[b]*Dipartimento di Scienze Ambientali, Università degli Studi della Tuscia, P.le dell'Università, 01100 Viterbo, Italy*
[c]*CNR, Istituto di Metodologie Chimiche, Area della Ricerca di Roma. C.P. 10, 00016 Monterotondo Stazione Roma, Italy*
[d]*Dipartimento di Scienze e Tecnologie Chimiche, Università degli Studi di Roma 'Tor Vergata', Via della Ricerca Scientifica 1, 00133 Roma, Italy*

Received 6 November 2007; accepted 29 November 2007

Abstract—The influence of the hydrophobic chain length on the chiral recognition capabilities of sodium *N*-acylprolinate micellar aggregates, used as biomembrane models, was investigated by ^{1}H NMR on the enantiomer couples of ditryptophan. The length of the hydrophobic portion of the surfactant is shown to influence the mode of enantiodiscrimination. Interestingly the hydrophobic chain length also affects the site of binding of heterochiral enantiomers as well as their conformation inside the aggregates.

1. Introduction

Chiral recognition plays a crucial role in the physico-chemical features of biological membranes as well as in their biological features controlled by the membrane organization.[1]

Biological membranes are formed by hundreds of different enantiopure components, lipids and proteins, that assemble and organize themselves in the lipid double layer according to the programme embedded in their molecular structure. The investigation of these remarkably complex systems relies on the use of models, such as micelles and liposomes, in which chemical composition and complexity are controlled. Many investigations have been carried out on models aimed at shedding some light on the modes by which chiral recognition manifests in these systems.[2] It has been shown that chiral recognition affects the organization and physico-chemical features of the aggregates, as well as the association of chiral solutes. However, some fundamental issues are not yet fully understood. It is currently unclear how the chiral information is translated from the monomeric components to the assembly, in which region or regions of the lipid double layer it is translated and expressed, and what is the role of the chiral function(s) in biological membranes.

Recently we reported that the enantiomer couples of ditryptophan **1** are discriminated by ^{1}H NMR in aggregates formed by sodium *N*-dodecanoyl-L-prolinate, **2a**, and that the heterochiral enantiomers (L-Trp-D-Trp, LD-**1** and D-Trp-L-Trp, DL-**1**) feature a site of association in the hydrophobic region of the aggregates, thus demonstrating that enantiodiscrimination takes place far from the functional groups of the stereogenic centres of the polar head groups, in the non-functionalized region of the aggregates.[2k] This evidence suggested to us that the combination of the monomer structure and self-assembling can translate the chiral information and hence the enantiodiscriminating capability to an entire region of the assembly, at a distance from the stereogenic centres, where recognition cannot be observed at the monomeric level.

The evidence of the expression of chirality in the hydrophobic part of the aggregates led us to investigate the role of the hydrophobic portion of a chiral amphiphile in the

* Corresponding authors. Tel.: +39 0761357052; fax: +39 0761357179 (S.B.); tel.: +39 0649913078; fax: +39 06490421 (G.M.); e-mail addresses: borocci@unitus.it; giovanna.mancini@uniroma1.it

0957-4166/$ - see front matter © 2007 Elsevier Ltd. All rights reserved.
doi:10.1016/j.tetasy.2007.11.035

transfer of chiral information from the monomer to the assembly and in the expression of chiral function by the assembly. Herein, we report an investigation carried out by ^{1}H NMR and molecular modelling on the chiral recognition of the four stereoisomers of ditryptophan (L-Trp-L-Trp, LL-**1**; D-Trp-D-Trp, DD-**1**; L-Trp-D-Trp, LD-**1**; D-Trp-L-Trp, DL-**1**), on their site of association, and on their conformation in aggregates formed by either sodium *N*-tetradecanoyl-L-prolinate, **2b** or sodium *N*-hexadecanoyl-L-prolinate, **2c** (Chart 1).

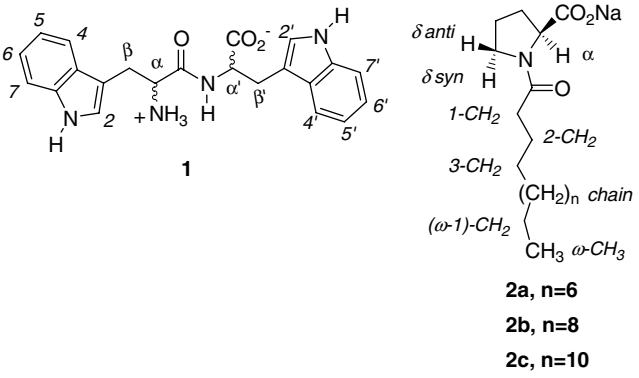

Chart 1.

2. Results and discussion

2.1. Preparation and characterization of surfactants

Surfactants **2b** and **2c** were prepared and purified according to a described procedure.[3] Their cmc and aggregation number, *n*, were measured by conductivity and fluorescence[4] experiments, respectively. In aggregating conditions, the isomers (*E* and *Z*) relative to the amidic bond organize in domains analogously to those previously reported for **2a**.[4c]

The values of cmc and *n*, reported in Table 1, show that the chain length influences the aggregation behaviour of sodium *N*-acylprolinates.

Table 1. Aggregation parameters of surfactants **2** measured at 298 K

Surfactant	cmc, M	*n*
2a	$(9.6 \pm 0.8) \times 10^{-2}$	46 ± 2[a]
2b	$(7.1 \pm 0.11) \times 10^{-4}$	60 ± 1
2c	$(2.4 \pm 0.12) \times 10^{-5}$	84 ± 5

[a] *n* value from Ref. 4c.

2.2. ^{1}H NMR recognition experiments

The dipeptide/aggregate interactions and the conformation of the dipeptides in the micellar aggregates have been investigated by 1D and 2D NMR experiments performed at 600.13 MHz. The aromatic region of the ^{1}H NMR spectra of the enantiomer couples of **1** (i.e., LL-**1**/DD-**1** and LD-**1**/DL-**1**) 20 mM in D_2O solutions of 94 mM **2b** or **2c** (in 100 mM phosphate buffer, pD = 5.8) are reported in Figures 1 and 2.

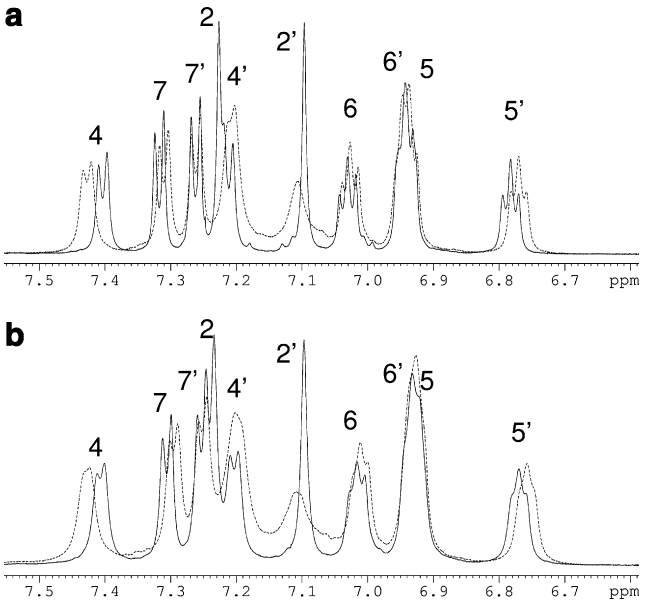

Figure 1. Comparison of the aromatic region of the 600.13 MHz ^{1}H NMR spectra of 20 mM LL-**1** (solid trace) and DD-**1** (dashed trace) in (a) 94 mM **2b**; (b) 94 mM **2c**. The spectra were performed in an aqueous buffered solution (100 mM phosphate buffer, pD = 5.8) at 300 K.

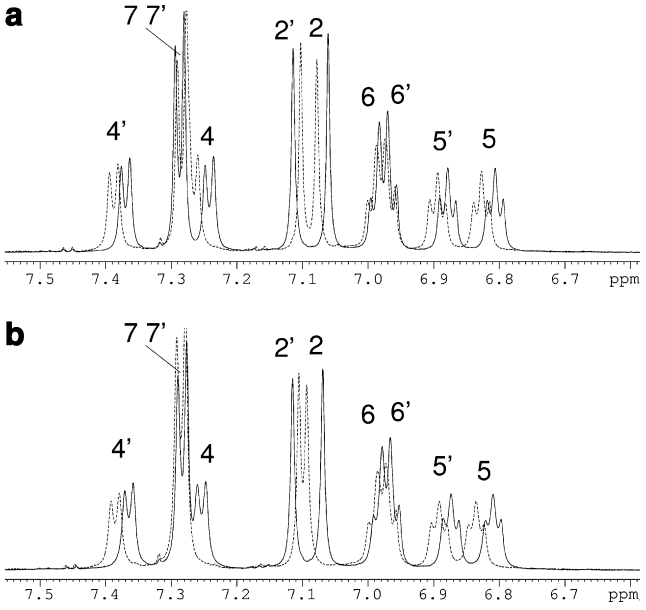

Figure 2. Comparison of the aromatic region of the 600.13 MHz ^{1}H NMR spectra of 20 mM LD-**1** (solid trace) and DL-**1** (dashed trace) in (a) 94 mM **2b**; (b) 94 mM **2c**. The spectra were performed in an aqueous buffered solution (100 mM phosphate buffer, pD = 5.8) at 300 K.

The complete assignment of the resonances due to ditryptophan, shown in Figures 1 and 2, has been performed as previously reported.[2k] The spectra of both LL-**1**/DD-**1** and LD-**1**/DL-**1** enantiomers are different because the

diastereomeric interactions with the chiral aggregates formed by either **2b** or **2c** yield different chemical shifts for some of the resonances; this is in analogy to what was observed previously in micellar aggregates of **2a**.

In Table 2, we report ^{1}H chemical shift differences of the resonances of homochiral (DD-**1** resonances subtracted from LL-**1** resonances) and heterochiral (DL-**1** resonances subtracted from LD-**1** resonances) couples of **1** in the presence of either **2b** or **2c**, compared to the chemical shift differences observed previously in the presence of **2a**.[2k] The values of chemical shift differences do not show any trend as a function of alkyl chain length, though the same couple of enantiomers is discriminated differently in the different aggregates, thus demonstrating the influence of chain length on the recognition process.

We also investigated the effect of the aromatic systems of **1** on the chemical shift of resonances due to surfactants, because it gives information on the site of the binding of **1** stereoisomers. The variations of chemical shifts observed in the ^{1}H NMR spectra of **2b** and **2c** aggregates due to the presence of the dipeptides are reported in Table 3, where they are compared with the corresponding variation previously observed in the spectra relative to **2a** aggregates.[2k] As observed in **2a** aggregates, the association of **1** isomers with **2b** and **2c** aggregates induces a remarkable upfield shift in some ^{1}H resonances due to the head groups of the *Z*-isomer of surfactants; in particular, signals due to the δ_Z^{syn} and δ_Z^{anti} protons are shifted upfield. Indeed, the corresponding protons of *E* isomers ($\delta_E^{syn}$and δ_E^{anti}) are less affected by the association with isomers **1**, because of the preferential binding of the dipeptides with the *Z*-domains of surfactants **2**. In analogy to what was observed in the aggregates of **2a**, the association of LL-**1** and DD-**1** enantiomers with the aggregates of **2b** and **2c** induces an upfield shift of resonances due to the surfactant head group protons (up to the third methylene of the alkyl chain) and a downfield shift of the resonances due to hydrophobic chain protons, demonstrating that the head groups and the hydrophobic alkyl chains are in the shielding and deshielding cone of the aromatic systems, respectively. This finding suggests the location of LL-**1** and DD-**1** in the head group region of the aggregates, independently of the chain length. On the other hand, there are some differences in the effect of the association of LD-**1** and DL-**1** enantiomers with

Table 2. ^{1}H chemical shift differences (Δ, Hz) for the enantiomer couples of **1** in the presence of micellar aggregates of surfactants **2**

	Δ, (Hz)					
	LL-**1** − DD-**1**			LD-**1** − DL-**1**		
Type	**2a**	**2b**	**2c**	**2a**	**2b**	**2c**
α	−4	1	5	−4	−2	−7
β	3	5	7	−14	−14	−17
2	8	18	17	−7	−10	−14
4	−16	−14	−13	−11	−16	−17
5	−4	−2	−5	−10	−13	−15
6	−2	2	3	−2	−2	−4
7	−2	4	6	1	−1	3
α′	1	−8	−9	8	13	13
β′	6	0	3	6	27	28
	0	6	11	—	7	5
2′	−5	−7	−6	6	7	6
4′	−8	5	3	−11	−10	−12
5′	7	7	7	−8	−9	−10
6′	−2	9	4	−44	0	−3
7′	−2	0	1	1	−1	−1

Table 3. Variation of chemical shift (in Hz) of the resolved resonances of ^{1}H NMR spectrum of surfactant **2** due to the presence of dipeptides **1**

Sample	α	δ_Z^{anti}	δ_E^{syn}	δ_E^{anti}	δ_Z^{syn}	1-CH_2	2-CH_2	3-CH_2	Chain	(ω-1)-CH_2	ω-CH_3
2a + DD-**1**	47	82	7	31	110	77	39	—	−5	—	−19
2b + DD-**1**	84	154	31	59	189	145	81	79	−13	−26	−25
2c + DD-**1**	87	155	32	56	187	144	84	87	−13	−21	−23
2a + LL-**1**	60	104	17	43	137	104	58	—	−8	—	−23
2b + LL-**1**	86	166	33	60	200	150	92	84	−14	−26	−26
2c + LL-**1**	85	164	36	58	193	146	97	86	−13	−17	−22
2a + LD-**1**	42	76	8	33	106	71	35	—	30	—	1
2b + LD-**1**	58	119	16	40	151	104	61	75	13	−7	−2
2c + LD-**1**	61	119	16	37	143	110	63	79	8	0	−2
2a + DL-**1**	35	78	7	29	101	74	37	—	28	—	1
2b + DL-**1**	52	128	16	37	151	110	61	75	12	−6	−2
2c + DL-**1**	51	121	17	32	136	110	60	79	8	−1	−2

Table 4. Interproton distances (in Å) obtained by ROESY cross peaks, and used as restrains in molecular mechanics calculation

Distance	In **2b** aggregates				In **2c** aggregates			
	LL-**1**	DD-**1**	LD-**1**	DL-**1**	LL-**1**	DD-**1**	LD-**1**	DL-**1**
β-4	3.2	3.3	3.1	3.0	3.7	3.9	3.2	3.1
β′-4′	3.1	3.6	3.0	3.3	3.3	4.0	3.1	3.5
α-4	2.7	2.9	2.9	3.0	2.8	3.1	2.9	2.9
α′-4′	3.4	4.8	3.3	3.2	3.5	—	3.3	3.1

surfactants **2** as a function of the chain length. All resonances due to the alkyl chain protons of **2a** were shifted upfield, whereas resonances due to the final hydrophobic fragment of **2b** and **2c** were shifted downfield. Moreover, the low upfield variation (lower with respect to that observed in **2a** spectrum) of the signal due to the main portion of the alkyl chain (Chain) is probably due to the downfield shift of some contributing resonances; therefore, some other protons of the final part of the alkyl chain of **2b** and **2c** should be in the deshielding cone of aromatic systems. Thus, the location of LD-**1** and DL-**1** enantiomers is generally shifted towards the hydrophobic region of the aggregates with respect to the location of LL-**1** and DD-**1**; however, the comparison of the three right columns of Table 3 relative to the LD-**1** and DL-**1** enantiomers shows that the different organizations of the aggregates, due to the different lengths of hydrophobic chain, influence the extent of their penetration in the hydrophobic region.

2.3. Calculation

We carried out a conformational search by means of molecular mechanics calculation using, as distance restraints, the experimental distances reported in Table 4, obtained by ROESY experiments.

The conformations obtained are reported in Figures 3 and 4. Figure 3 shows that in the aggregates of **2b** and **2c**, LL-**1** and DD-**1** enantiomers have the same 'folded conformation', where the aromatic systems of the amino acid residues are arranged in a parallel mode, analogous to that previously found in **2a**.[2k] Figure 4 shows that, on the other hand, the LD-**1** and DL-**1** isomers feature in both **2b** and **2c** aggregates a 'folded conformation', where the aromatic systems are not parallel, and that this conformation is completely different from the 'defolded conformation' previously found in the aggregates of **2a** and also reported for comparison in Figure 4e and f. The chain length and the corresponding different organization of the aggregates im-

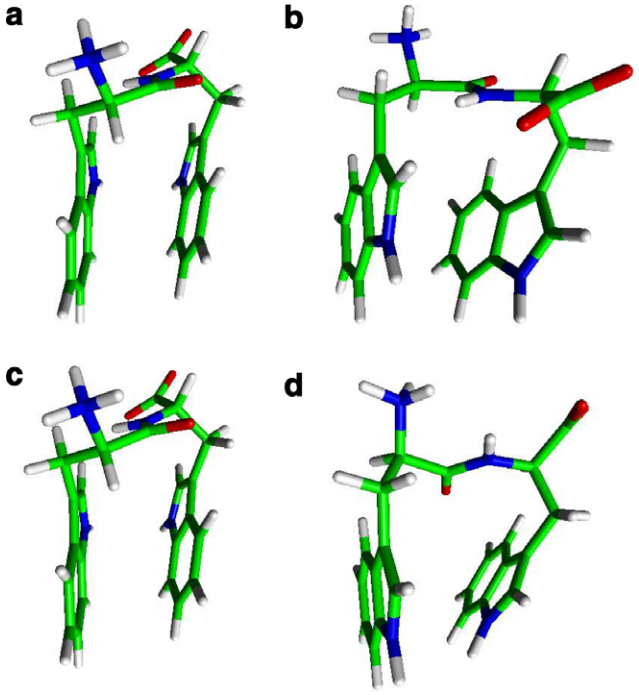

Figure 3. Conformation obtained by molecular mechanics calculation relative to (a) LL-**1** in aggregates of **2b**; (b) DD-**1** in aggregates of **2b**; (c) LL-**1** in aggregates of **2c**; (d) DD-**1** in aggregates of **2c**.

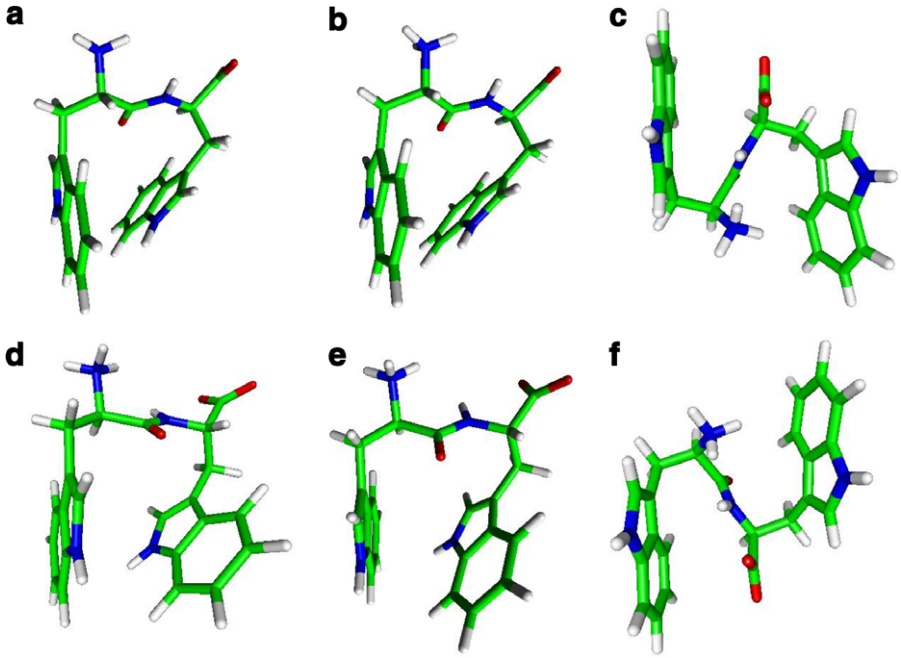

Figure 4. Conformation obtained by molecular mechanics calculation relative to (a) LD-**1** in aggregates of **2b**; (b) LD-**1** in aggregates of **2c**; (c) LD-**1** in aggregates of **2a**; (d) DL-**1** in aggregates of **2b**; (e) DL-**1** in aggregates of **2c**; (f) DL-**1** in aggregates of **2a**.

pose a different site of binding and a different conformation to the LD-**1** and DL-**1** isomers.

The different conformation and the correspondingly different relative position of the aromatic systems of LD-**1**/DL-**1** amino acid residues should influence the chemical shift of resonances due to aromatic protons. Actually, in the 'defolded conformation', as observed in **2a** aggregates (Fig. 4c and f), the aromatic systems are far from each other whereas in the 'folded conformation', as observed in aggregates of **2b** and **2c** (Fig. 4a, b and d, e), the shielding cone of one system should influence the resonances of the second system protons and vice versa. Thus, the different conformation should influence the chemical shift difference between the corresponding protons of the two amino acid residues (i.e., 2-2′, 4-4′, ...) in the conformation of LD-**1** and DL-**1** found in **2b**/**2c** aggregates with respect to the conformation of the same dipeptides found in **2a**.

Since the effect of ring current can be better detected in the absence of specific interactions we calculated the ^{1}H NMR spectra of both the conformations found for LD-**1** by DFT calculation in vacuum,[5] and made a comparison between experimental and calculated spectra. In the experimental spectra, the most relevant variation concerns the 2-2′ chemical shift difference in the spectra of LD-**1** and DL-**1** enantiomers obtained in the presence of **2b** and **2c** with respect to those obtained in the presence of **2a** (Table 5). In the calculated spectra, there are variations between the 'defolded' and the 'folded' conformation in the 2-2′ (−470 Hz vs 360 Hz) 5-5′ (36 Hz vs 121 Hz) and 7-7′ (−24 Hz vs 249 Hz) chemical shift differences. The fact that in both the calculated and experimental spectra, the largest variation concerns the 2-2′ chemical shift difference supports the different conformations of LD-**1** and DL-**1** enantiomers obtained in the presence of **2b** and **2c** with respect to **2a**. We believe that the very close value of the experimental chemical shift differences between the corresponding protons of amino acid residues of LL-**1** and DD-**1** in all **2** aggregates (reported in Table 5) confirms the validity of this approach to support the consistency of LD-**1** and DL-**1** conformations found by ROESY experiments and molecular mechanics calculation.

Table 5. Chemical shift differences (in Hz) between the signals of the corresponding protons of the dipeptide amino acid residues in the ^{1}H NMR spectra

Sample	2-2′	4-4′	5-5′	6-6′	7-7′
LL-**1** in **2a**	67	110	89	50	31
LL-**1** in **2b**	78	115	97	48	33
LL-**1** in **2c**	83	122	92	50	32
DD-**1** in **2a**	54	119	100	50	30
DD-**1** in **2b**	53	134	107	55	29
DD-**1** in **2c**	59	138	105	52	26
LD-**1** in **2a**	−47	−84	−40	13	0
LD-**1** in **2b**	−32	−77	−43	10	0
LD-**1** in **2c**	−28	−67	−39	10	0
DL-**1** in **2a**	−34	−86	−37	13	0
DL-**1** in **2b**	−15	−71	−40	10	0
DL-**1** in **2c**	−8	−62	−34	11	−4

3. Conclusions

The influence of chain length on the chiral recognition capabilities of sodium *N*-acyl-L-prolinates was investigated by NMR, molecular mechanics calculation, and ab initio calculation using the four stereoisomers of ditryptophan as probes of chirality. The chain length influences the aggregating behaviour of the surfactants, as expected, but it also influences their enantiodiscriminating capabilities because enantiomers are discriminated differently in the different aggregates. Moreover, the specific interactions with the different aggregates control the extent of penetration of heterochiral enantiomers in the hydrophobic region of the aggregates and determine the variation of their conformation within aggregates of **2b** and **2c** with respect to the conformation previously found in aggregates of **2a**.[2k] The observation of the enantiodiscrimination of LD-**1** and DL-**1** enantiomers in concurrence with the evidences of their site of binding remote from the head group stereogenic centres confirms that in the aggregation, the chiral information and the discriminating capability are translated from the monomer to entire regions of the aggregates, at distances from the stereogenic centres where chiral recognition cannot be observed at the monomeric level. The recognition processes concerning enantiodiscrimination and the variation of conformation occurring in the hydrophobic region demonstrate that this zone, although governed by Van der Waals interactions, features a high extent of organization imprinted by the monomer structure via selfassembling.

4. Experimental

4.1. Materials

Sodium *N*-tetradecanoyl-L-prolinate **2b** and sodium *N*-hexadecanoyl-L-prolinate **2c** were prepared and purified as previously described.[3]

The LL/DD enantiomer couple of ditryptophan **1** was purchased from Research Plus Inc. and used as such. The other two **1** isomers, LD-**1** and DL-**1**, were prepared as previously described.[2k] D_2O (100% atom D) was purchased from Armar Chemicals. All other reagents of the highest purity grade were purchased from Fluka or Sigma–Aldrich.

4.2. Characterization of surfactants

The critical micellar concentration (cmc) of surfactants **2** was measured, at 298 K by conductivity measurements on solutions obtained by adding known volumes of a concentrated aqueous solution of surfactant (25 mM and 5 mM for **2b** and **2c**, respectively) to a known volume of bidistilled water; measurements were carried out on an Hanna conductimeter, HI-9932, equipped with a thermostating apparatus.

The aggregation number of aggregates, n, formed by **2b** and **2c** was measured by fluorescence experiments, according to a described procedure, using 4-(1-pyrenil)-butanoic

acid and hexadecylpyridinium chloride as fluorescent probe and quencher, respectively.[4]

4.3. Sample preparation

A 100 mM sodium phosphate buffer in D_2O was used to prepare all solutions considered in this investigation (pD = 5.8).

Solutions of dipeptides were prepared by dissolving 5.46 mg of **1** in 700 μL (20 mM) of 94 mM micellar solution directly into the NMR sample.

4.4. NMR experiments

1D and 2D NMR experiments were performed on a Bruker AVANCE AQS600 spectrometer operating at 600.13 MHz and 150.92 MHz for the ^1H and ^{13}C Larmor frequency, respectively. The spectrometer was equipped with a Bruker multinuclear inverse probe head. ^1H NMR spectra were referenced with respect to the residual proton signal of D_2O ($\delta = 4.780$ ppm at 300 K). All 1D experiments were performed without suppression of the residual HDO signal. The spectral assignment was performed using conventional 2D experiments as previously reported.[2k]

ROESY (rotating frame Overhauser enhancement spectroscopy) experiments were performed in the TPPI phase sensitive mode with a spectral sweep width of 6 kHz in both dimensions, 1024 data points in f_2 and 512 increments in f_1, and a recycle delay of 2 s. A mixing time of 80 ms was used, and mixing was achieved by the continuous wave method with a field strength of 5 kHz. Zero filling in f_1 to 1024 real data points and 90° phase-shifted square-sine bell window functions in both dimensions were applied before Fourier transformation.

4.5. Determination of dipeptide intramolecular distances

Inter-proton distances were obtained by integration of the cross-peaks in the ROESY spectra as previously described in an analogous investigation.[2k]

4.6. Calculation

4.6.1. Conformational search. Molecular mechanics calculations were performed with the MacroModel 6.0 package[6] running on a Silicon Graphics O2 R10000 workstation, and using AMBER* force field. The electrostatic interactions were evaluated using the partial atomic charges of the AMBER* force field,[7] and a dielectric constant of 10 was used to reproduce the micellar medium.[8] A conformational search with distance restrains was carried out on the molecular structures of the four stereoisomers of ditryptophan as previously described.[2k]

4.6.2. Ab initio calculation. A density functional theory (DFT) approach was used for calculating the ^1H NMR chemical shifts of LD-**1** different conformations, according to a previously described procedure.[5] The geometries of the minimum energy conformation in **2a** and **2b**, obtained by a restrained conformational search, were used as initial structures for the DFT calculation. The geometries were optimized in vacuum by using the hybrid exchange correlation functional B3LYP,[9] in conjunction with the 6-31G(d,p) basis set, with a constrain on the dihedral angles ϕ, ψ, χ_1, χ_2 of both residues. The nuclear shieldings were calculated in vacuum at the B3LYP/cc-pVTZ level of theory and converted in chemical shifts by referencing them to TMS ($\delta = \sigma_{TMS} - \sigma$). The DFT calculation was performed using the Unix version of the GAUSSIAN 03[10] running on a HP Proliant DL585 machine.

Acknowledgements

This work has been carried out in the frame of the project 'The use of surfaces and vesicles for the amplification of homochirality in polypeptide chains' of COST action D27. We acknowledge the contribution from CNR, Dipartimento di Progettazione Molecolare.

References

1. (a) Fadok, V. A.; de Cathelineau, A.; Daleke, D. L.; Henson, P. M.; Bratton, D. L. *J. Biol. Chem.* **2001**, *276*, 1071–1077; (b) Cohen, M.; Joester, D.; Geiger, B.; Addadi, L. *Chem. Biochem.* **2004**, *5*, 1393–1399.
2. (a) Arnett, E. M.; Thompson, O. *J. Am. Chem. Soc.* **1981**, *103*, 968–970; (b) Arnett, E. M.; Gold, J. M. *J. Am. Chem. Soc.* **1982**, *104*, 636–639; (c) Fuhrop, J. H.; Schnieder, P.; Rosenberg, J.; Boekema, E. *J. Am. Chem. Soc.* **1987**, *109*, 3387–3390; (d) Pathirana, S.; Neely, W. C.; Myers, L. J.; Vodyanoy, V. *J. Am. Chem. Soc.* **1992**, *114*, 1404–1405; (e) Morigaki, K.; Dallavalle, S.; Walde, P.; Colonna, S.; Luisi, P. L. *J. Am. Chem. Soc.* **1997**, *119*, 292–301; (f) Walde, P.; Blöchliger, E. *Langmuir* **1997**, *13*, 1668–1671; (g) Uragami, M.; Miyake, Y.; Regen, S. L. *Langmuir* **2000**, *16*, 3491–3496; (h) Lalitha, S.; Kumar, A. S.; Stine, K. J.; Covey, D. F. J. *Supramol. Chem.* **2001**, *1*, 53–61; (i) Borocci, S.; Ceccacci, F.; Galantini, L.; Mancini, G.; Monti, D.; Scipioni, A.; Venanzi, M. *Chirality* **2003**, *15*, 441–447; (j) Nakagawa, H.; Yoshida, M.; Kobori, Y.; Yamada, K.-I. *Chirality* **2003**, *15*, 703–708; (k) Bombelli, C.; Borocci, S.; Lupi, F.; Mancini, G.; Mannina, L.; Segre, A. L.; Viel, S. *J. Am. Chem. Soc.* **2004**, *126*, 13354–13362; (l) Andreani, R.; Bombelli, C.; Borocci, S.; Lah, J.; Mancini, G.; Mencarelli, P.; Vesnaver, G.; Villani, C. *Tetrahedron: Asymmetry* **2004**, *15*, 987–994; (m) Epand, R. M.; Rychnovsky, S. D.; Belani, J. D.; Epand, R. F. *Biochem. J.* **2005**, *390*, 541–548; (n) Nakagawa, H.; Onoda, M.; Masuoka, Y.; Yamada, K.-I. *Chirality* **2006**, *18*, 212–216; (o) Cruciani, O.; Borocci, S.; Lamanna, R.; Mancini, G.; Segre, A. L. *Tetrahedron: Asymmetry* **2006**, *17*, 2731–2737; (p) Ceccacci, F.; Giansanti, L.; Mancini, G.; Mencarelli, P.; Sorrenti, A. *New J. Chem.* **2007**, *31*, 86–92.
3. Takehara, M.; Yoshimura, I.; Takizawa, K.; Yoshida, R. *J. Am. Oil Chem. Soc.* **1972**, *49*, 157–161.
4. (a) Infelta, P.; Grätzel, M. *J. Chem. Phys.* **1979**, *70*, 179–186; (b) Alargova, R. G.; Kochijashky, I. I.; Sierra, M. L.; Zana, R. *Langmuir* **1998**, *14*, 5412–5418; (c) Amenitsch, H.; Bombelli, C.; Borocci, S.; Ceccacci, F.; Mancini, G.; Rappolt, M. *J. Coll. Interface Sci.* **2004**, *280*, 212–218.
5. Bagno, A. *Chem. Eur. J.* **2001**, *7*, 1652–1661, and references therein.
6. Mohamadi, F.; Richards, N. G. J.; Guida, W. C.; Liskamp, R.; Lipton, M.; Caufield, C.; Chang, G.;

Hendrikson, T.; Still, W. C. *J. Comput. Chem.* **1990**, *11*, 440–467.
7. (a) Weiner, S. J.; Kollman, P. A.; Case, D. A.; Singh, U. C.; Ghio, C.; Alagona, G.; Profeta, S., Jr.; Weiner, P. *J. Am. Chem. Soc.* **1984**, *106*, 765–784; (b) McDonald, D. Q.; Still, W. C. *Tetrahedron Lett.* **1992**, *33*, 7747–7750.
8. (a) Bunton, C. A.; Minch, M. J.; Hildago, J.; Sepulveda, L. *J. Am. Chem. Soc.* **1973**, *95*, 3262–3272; (b) Carpenter, K. A.; Wilkes, B. C.; Weltrowska, G.; Schiller, P. W. *Eur. J. Biochem.* **1996**, *241*, 756–764.
9. (a) Becke, A. D. *Phys. Rev. A* **1988**, *38*, 3098–3100; (b) Becke, A. D. *ACS Symp. Ser.* **1989**, *394*, 165–179; (c) Becke, A. D. *J. Chem. Phys.* **1993**, *98*, 5648–5652; (d) Lee, C.; Yang, W.; Parr, R. G. *Phys. Rev. B* **1988**, *37*, 785–789.
10. Frisch, M. J.; Trucks, G. W.; Schlegel, H. B.; Scuseria, G. E.; Robb, M. A.; Cheeseman, J. R.; Zakrzevski, V. G.; Montgomery, J. A., Jr.; Vreven, T.; Kudin, K. N.; Burant, J. C.; Millam, J. M.; Iyengar, S. S.; Tomasi, J.; Barone, V.; Mennucci, B.; Cossi, M.; Scalmani, G.; Rega, N. G.; Petersson, G. A.; Nakatsuji, H.; Hada, M.; Ehara, M.; Toyota, K.; Fukuda, R.; Hasegawa, J.; Hishida, M.; Nakajima, T.; Honda, Y.; Kitao, O.; Nakai, H.; Klene, M.; Li, X.; Knox, J. E.; Hratchian, H. P.; Cross, J. B.; Adamo, C.; Jaramillo, J.; Gomperts, R.; Stratman, R. E.; Yazyev, O.; Austin, A. J.; Cammi, R.; Pomelli, C.; Ochterski, J. W.; Ayala, P. Y.; Morokuma, K.; Voth, G. A.; Salvador, P.; Dannenberg, J. J.; Zakrzewski, V. G.; Dapprich, S.; Daniels, A. D.; Strain, M. C.; Farkas, O.; Malick, D. K.; Rabuck, A. D.; Raghavachari, K.; Foresman, J. B.; Ortiz, J. V.; Cui, Q.; Baboul, A. G.; Clifford, S.; Cioslowski, J.; Stefanov, B. B.; Liu, G.; Liashenko, A.; Piskorz, P.; Komaromi, I.; Martin, R. L.; Fox, D. J.; Keith, T.; Al-Laham, M. A.; Peng, C. Y.; Nanayakkara, A.; Challacombe, M.; Gill, P. M. W.; Johnson, B. G.; Chen, W.; Wong, M. W.; Gonzalez, C.; Pople, J. GAUSSIAN 03, Revision C.02; Gaussian: Wallingford, CT, 2004.